

SINTERING BEHAVIOR OF PLASMA-SPRAYED $\text{Sm}_2\text{Zr}_2\text{O}_7$ COATING

Jianhua Yu, Huayu Zhao, Shunyan Tao*, Xiaming Zhou, Chuanxian Ding

Key laboratory of inorganic coating materials, Chinese Academy of Sciences, Shanghai 200050, China
Shanghai Institute of Ceramics, Chinese Academy of Sciences, Shanghai 200050, China

ABSTRACT

Plasma-sprayed thermal barrier coating (TBC) systems are widely used in gas turbine blades to increase turbine entry temperature (TET) and better efficiency. Yttria stabilized zirconia (YSZ) has been the conventional thermal barrier coating material because of its low thermal conductivity, relative high thermal expansion coefficient and good corrosion resistance. However the YSZ coatings can hardly fulfill the harsh requirements in future for higher reliability and the lower thermal conductivity at higher temperatures. Among the interesting TBC candidates, materials with pyrochlore structure show promising thermo-physical properties for use at temperatures exceeding 1200 °C. $\text{Sm}_2\text{Zr}_2\text{O}_7$ bulk material does not only have high temperature stability, sintering resistance but also lower thermal conductivity and higher thermal expansion coefficient. The sintering characteristics of ceramic thermal barrier coatings under high temperature conditions are complex phenomena. In this paper, samarium zirconate ($\text{Sm}_2\text{Zr}_2\text{O}_7$, SZ) powder and coatings were prepared by solid state reaction and atmosphere plasma spraying process, respectively. The microstructure development of coatings derived from sintering after heat-treated at 1200–1500 °C for 50 h have been investigated. The microstructure was examined by scanning electron microscopy (SEM) and the grain growth was analyzed in this paper as well.

INTRODUCTION

Plasma sprayed ceramic thermal barrier coatings (TBCs) are widely applied for protecting hot-section metal components of gas turbines from combustion gases. The state-of-the-art TBCs is based on zirconia-based materials especially 7–8 wt% Y_2O_3 stabilized zirconia (YSZ) because of its low thermal conductivity and good mechanical properties [1–4]. However, the application of YSZ limits to 1200 °C for long-term service due to phase transformations from the t'-tetragonal to tetragonal and cubic (t+c) and then to monoclinic (m) zirconia. The phase transformations cause a volume change which leads

to the formation of cracks and early degradation of the coating during cooling [5]. In addition, decrease in the strain compliance associated with sintering in the application also results in degradation of the YSZ coating [6–9]. Operations at higher temperatures are needed for TBC to further increase the efficiency and durability of gas turbines. Therefore, more and more efforts have been devoted to the development of new TBC materials. The rare-earth zirconates- $\text{Ln}_2\text{Zr}_2\text{O}_7$ (Ln-La, Nd, Sm and Gd) with a pyrochlore structure are attractive because of their lower thermal conductivity and better thermal stability compared with YSZ [10–14].

Thermo-physical properties of bulk materials showed that the thermal conductivity of $\text{Sm}_2\text{Zr}_2\text{O}_7$ (abbreviated as SZ) was low and the thermal expansion coefficient of SZ was relatively high [15]. In addition, electron-beam directed-vapor deposited SZ coating has been examined by Zhao [16]. The thermal conductivity and mechanical properties of TBC depends on its microstructure, and the microstructure of plasma sprayed coatings is sensitive to high temperature exposure during operation. The reconfiguration of microstructure, caused by sintering, involving microcrack healing, pore shape change and the grain growth contributes to increase in thermal conductivity of plasma sprayed TBC, and makes it ineffective in protection of metallic material. Moreover, increase in elastic modulus associated with sintering also leads to decrease cycling life of the TBC.

In this work, SZ powder and coatings were prepared by solid-state reaction and plasma spraying, respectively. The microstructure of SZ coating was examined. The microstructure development and grain growth of SZ coating during heat treatments at 1200–1500 °C for 50 h were also performed.

EXPERIMENTAL PROCEDURE

Materials and Preparation

SZ powder was synthesized by solid state reaction. Sm_2O_3 and ZrO_2 powders were used as starting materials, which are mixed with the stoichiometric ratios. An ethanol-based

*Professor and author of correspondence

suspension of the mixture was ball-milled for 12 h with zirconia balls and dried. After drying, the mixture was calcined at 1550 °C for 5 h to obtain a pyrochlore structured powder [17], then ball-milled, granulated and sieved for plasma spraying.

The coatings were deposited by the PT-A2000 atmospheric plasma spraying system equipped with an F4-MB plasma gun (Sulzer Metco AG, Wohlen, Switzerland). Primary and auxiliary plasma gases were Ar and H₂. The former was also used to act as a powder carrier gas. Detailed spraying parameters can be found in our publication [17]. To obtain free-standing samples used in this work, coatings were deposited onto an aluminium substrate and removed from the substrate by grinding the substrate off.

Specimen Characterization

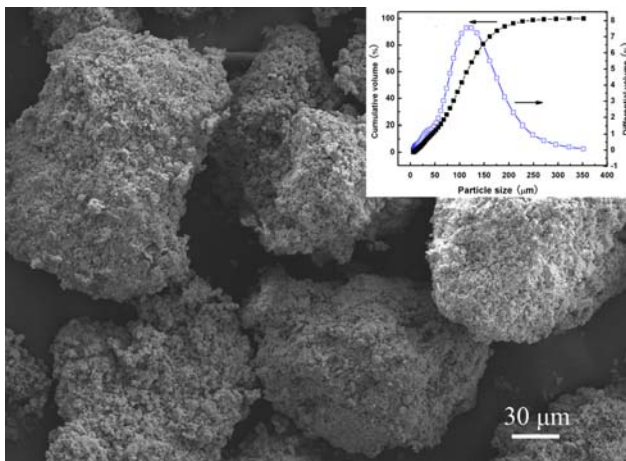


Figure 1. Morphology and particle size distribution of SZ powder for plasma spraying

The morphology of the feedstock and coatings was examined employing an EMPA-8705 QH2 electron probe analyzer (Shimadzu, Tokyo, Japan) with affiliated energy-dispersive spectrometer detector (EDS). The particle size distribution was explored by Microtrac S3500 Particle Size Analyser (Nikkiso, Japan). The median size (D_{50}) of SZ powder is 102.2 μm. Figure 1 represents the morphology and particle size distribution of SZ powder. The density of SZ coatings was measured by the Archimedes method with an immersion medium of deionized water.

For grain growth studies, the free-standing SZ coating was cut with dimension of 2mm×2mm×1mm, then the surface of the sample was polished, and the polished samples were heat treated for 50 h at 1200, 1300, 1400, 1500 °C, and for 10, 30, 50, 80, 100 h at 1400 °C, respectively. The subsequent heat treatment performed as a thermal etching process to reveal the grain boundaries of the coating. The grain size and distribution were analyzed from SEM micrographs by image analysis software (Image Pro Plus, Media Cybernetics) using a line-intercept method and taking into account at least 200 grains.

RESULTS AND DISCUSSIONS

Microstructure Analysis

Figure 2 shows the fracture surfaces of the as-sprayed SZ coating. A typical lamellar structure for plasma spraying was observed, which is formed by over-lapping of individual splats aligned predominantly parallel to the substrate surface, and the relative density was 87.2%. It was observed (in Fig. 2) that the grain structure within individual splats was columnar. Microcracks and pores arising from poor adhesion between splats and entrapped gases, respectively, were also presented.

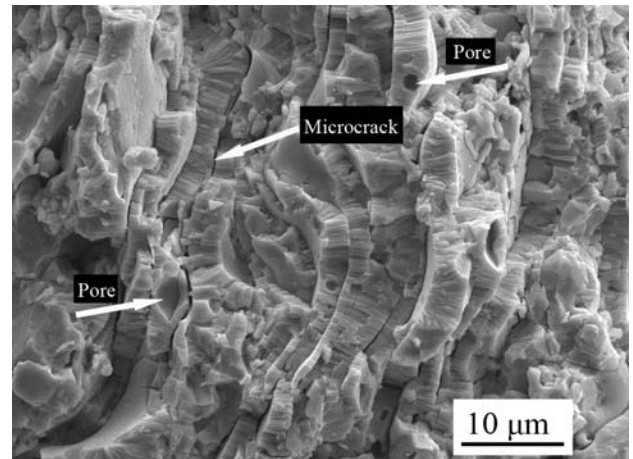


Figure 2. SEM micrographs of the fracture surface of the as-sprayed SZ coating

The typical microstructure of plasma sprayed SZ coatings after heat treatment at 1300 °C and 1500 °C for 50 h is shown in Fig. 3. It is obvious that most splat interfaces disappeared after heat treatment at 1500 °C for 50 h, the columnar structure exhibited in Fig. 2 is not observed, and globular voids are dominant in the coatings after heat treatments. The disappearance of the inter-splat boundaries after heat treatments would contribute to an increase in thermal conductivity [17].

Sintering Behavior

The SEM micrographs of SZ coatings heat treated at 1400 °C for 10 h and 100 h are shown in Fig.4 (a-b). It was observed that the grain has an obvious growth, and the grain size of SZ coatings is shown in Table 3. It shows that the average grain size increased from 0.64 μm for 10 h to 1.34 μm for 100 h. As the sintering occurs, the grain boundary and surface diffusion lead to grain growth. Meanwhile the average grain size of coatings after heat treatments for 50 h at different temperatures is presented in Table 4. The average grain size increased from 0.50 μm to 1.93 μm with rise in heat treatment temperature from 1200 °C to 1500 °C, suggesting that the grain growth is more sensitive to temperature than time.

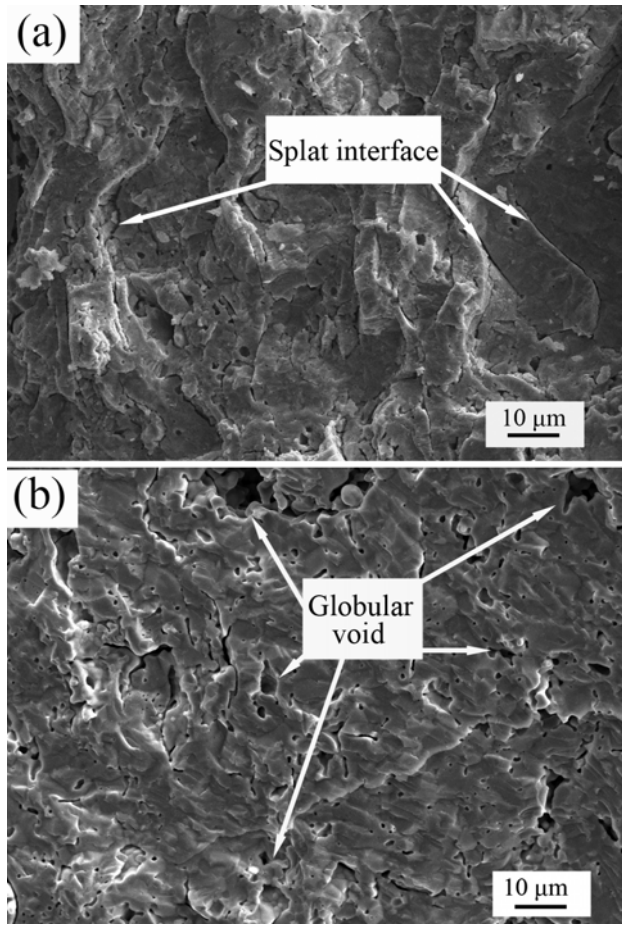


Figure 3. SEM micrographs of the fracture surface of SZ coatings heat treated at 1300 (a) and 1500 °C (b) for 50 h

Table 1 Grain size of SZ coatings heat treated at 1400 °C for different periods

Time (h)	10	30	50	80	100
Grain size (μm)	0.64±0.03	0.97±0.05	1.01±0.05	1.24±0.06	1.34±0.07

Table 2 Grain size of SZ coatings heat treated for 50 h at different temperatures

Temperature (°C)	1200	1300	1400	1500
Grain size (μm)	0.5±0.02	0.62±0.03	1.01±0.05	1.93±0.10

The grain size with a function of aging time t could be described as:

$$d - d_0 = kt^{1/2} \quad (1)$$

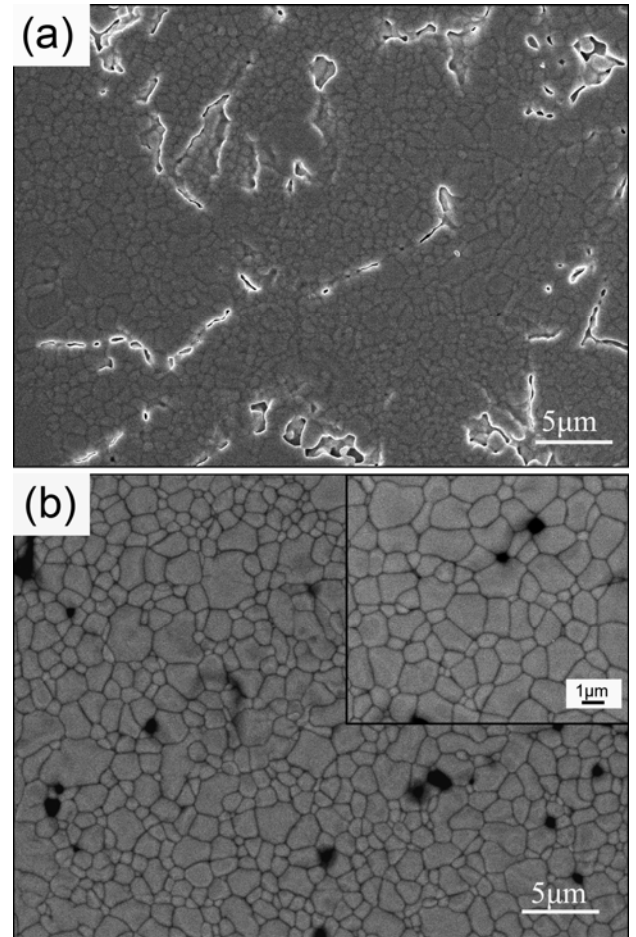


Figure 4. SEM micrographs of SZ coatings heat treated at 1400 °C for (a) 10 h, (b) 100 h

where d_0 and d are, respectively, the grain size before and after heat treating for t (time—expressed in s), and k is a proportionality coefficient which has a relationship with the activation energy E , similar to that of diffusion, because the atomistic process necessary for grain growth is the jumping of an atom from one side of a boundary to the other as a diffusional jump in the boundary, as followings:

$$k = k_0 e^{-\frac{E}{RT}} \quad (2)$$

where R is the universal gas constant and k_0 is a constant. d_0 was estimated to be 0.35 μm calculated by the fitting data in Table 1 (grain size) through Fig.5a, and then the equation (2) and value of d_0 were taken into the equation (1), a new equation (3) was obtained.

$$d - d_0 = k_0 e^{-\frac{E}{RT}} t^{1/2} \quad (3)$$

The activation energy of grain growth within the plasma-sprayed SZ coating was deduced from Fig. 5b (using the values in Table 2) which shows the variation of $\ln(d-d_0)$ with minus reciprocal of temperature. Hence, the activation energy of grain growth is calculated to be approximate 178 kJmol^{-1} which is higher than that of YSZ coatings obtained from creep measurements (104 kJmol^{-1} [18]).

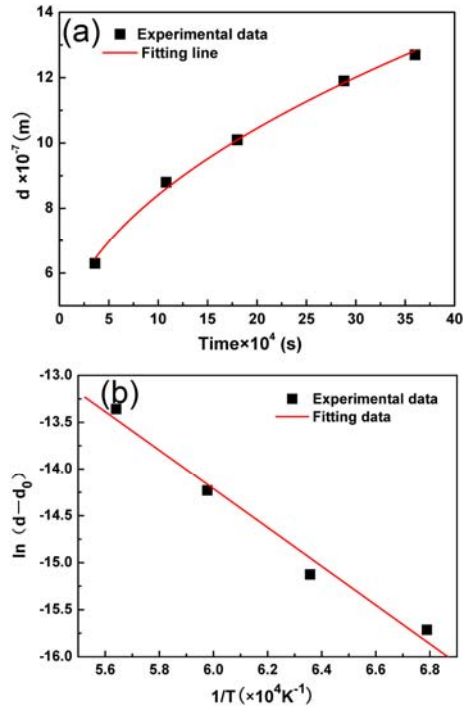


Figure 5: (a) Grain size with heat treatment period at $1400 \text{ }^\circ\text{C}$, (b) Variation of $\ln(d-d_0)$ with reciprocal of temperature.

CONCLUSIONS

SZ coating was deposited by plasma spraying using powders obtained by solid-state reaction. A typical layered structure SZ coating with columnar grains in individual splats was investigated. After high temperature exposure ($1500 \text{ }^\circ\text{C}$ for 50 h), inter-splat cracks and columnar grain structure observed in as-sprayed coatings disappeared. In addition, the activation energy of grain growth for plasma sprayed SZ coatings was 178 kJmol^{-1} , which is higher than that of YSZ, implying a good sintering resistance for SZ coatings. Therefore, SZ might be a potential candidate for thermal barrier coating application.

REFERENCES

[1] Miller, R.A., 1987, "Current Status of Thermal Barrier Coatings—An Overview", *Surface and Coatings Technology*, Vol. **30**, pp. 1–11.
 [2] Tamura, M., Takahashi, M., Ishii, J., Suzuki, K., Sato M. and Shimomura, K., 1999, "Multilayered Thermal Barrier Coating for Land-Based Gas Turbines", *Journal of Thermal Spray Technology*, Vol. **8**(1), pp. 68–72.

[3] Miller, R.A., 1984, "Oxidation-Based Model for Thermal Barrier Coating Life", *Journal of the American Ceramic Society*, Vol. **67**(8), pp. 517–521.
 [4] Khor K.A. and Gu Y.W, 2000, "Thermal Properties of Plasma-Sprayed Functionally Graded Thermal Barrier Coatings", *Thin Solid Films*, Vol. **372**, pp. 104–113.
 [5] Miller, R. A., Smialek, J.L. and Garlick, R.G., 1981, "Phase stability in plasma-sprayed partially stabilized Zirconia-Yttria, in *Advances in Ceramics*", Vol. 3, *Science and Technology of Zirconia*. In A.H.Heuer and L.W.Hobbs, ed., American Ceramic Society, Columbus, OH, pp. 241–251.
 [6] Huang, H., Eguchi K., and Yoshida, T., 2003, "Novel Structured Yttria-Stabilized Zirconia Coatings Fabricated by Hybrid Thermal Plasma Spraying", *Science and Technology of Advanced Materials*, Vol. **4**, pp. 617–622.
 [7] Zhu, D.M. and Miller, R.A., 1998, "Sintering and Creep Behavior of Plasma-Sprayed Zirconia- and Hafnia-Based Thermal Barrier Coatings", *Surface and Coatings Technology*, Vol. **108–109**(1–3), pp. 114–120.
 [8] Clarke, D.R. and Levi, C.G., 2003, "Materials Design for the Next Generation Thermal Barrier Coatings", *Annual Reviews of Materials Research*, Vol. **33**, pp. 383–417.
 [9] Renteria, A.F. and Saruhan, B., 2006, "Effect of Ageing on Microstructure Changes in EB-PVD Manufactured Standard PYSZ Top Coat of Thermal Barrier Coatings", *Journal of the European Ceramic Society*, Vol. **26**, pp. 2249–2255.
 [10] Pan, W., Wan, C.L., Xu, Q., Wang, J.D. and Qu, Z.X., 2007, "Thermal Diffusivity of Samarium-Gadolinium Zirconate Solid Solutions", *Thermochimica Acta*, Vol. **455**, pp. 16–20.
 [11] Lehmann, H., Pitzer, D., Pracht, G., Vassen, R. and Stover, D., 2003, "Thermal Conductivity and Thermal Expansion Coefficients of the Lanthanum Rare-Earth-Element Zirconate System", *Journal of the American Ceramic Society*, Vol. **86**, pp. 1338–1344.
 [12] Wu, J., Wei, X., Padture, N.P., Klemens, P.G., Gell, M., Garcia, E., Miranzo, P. and Osendi, M.I., 2002, "Low Thermal Conductivity Rare-Earth Zirconates for Possible Thermal- Barrier Coatings Application", *Journal of the American Ceramic Society*, Vol. **85**, pp. 3031–3035.
 [13] Vassen, R., Cao, X., Tietz, F., Basu, D. and Stöver, D., 2000, "Zirconates as New Materials for Thermal Barrier Coatings", *Journal of the American Ceramic Society*, Vol. **83**, pp. 2023–2028.
 [14] Subramanian, R., 2001, "Thermal Barrier Coating Having High Phase Stability", US Patent 6258467, Siemens Westinghouse Power Corporation (Orlando, FL).
 [15] Liu, Z.G., Ouyang, J.H. and Zhou, Y., 2009, "Structural

Evolution and Thermophysical Properties of $(\text{Sm}_x\text{Gd}_{1-x})_2\text{Zr}_2\text{O}_7$ ($0 \leq x \leq 1.0$) ceramics”, *Journal of Alloys and Compounds*, Vol. **472**, pp. 319–324.

[16] Zhao, H.B., Levi C.G. and Wadley H. N.G., 2009, “Vapor Deposited Samarium Zirconate Thermal Barrier Coatings,” *Surface and Coatings Technology*, Vol. **203**, pp. 3157–3167.

[17] Yu, J.H, Zhao, H.Y., Tao, S.Y., Zhou, X.M. and Ding,

C.X., 2010, “Thermal conductivity of plasma sprayed $\text{Sm}_2\text{Zr}_2\text{O}_7$ coatings”, *Journal of the European Ceramic Society*, Vol. **30**, pp.799–804.

[18] Zhu, D.M. and Miller, R.A., “Determination of Creep Behavior of Thermal Barrier Coatings Under Laser Imposed Temperature and Stress Gradients,” NASA Technical Memorandum 113169 ARL-TR-1565, November; 1997.